ELSEVIER

Journal of Alloys and Compounds 446–447 (2007) 232–236

Journal of ALLOYS AND COMPOUNDS

www.elsevier.com/locate/jallcom

On the local structure of Ti during in situ desorption of $Ti(OBu)_4$ and $TiCl_3$ doped $NaAlH_4$

Cornelis P. Baldé [a], Ad M.J. van der Eerden [a], Hans A. Stil [b], Frank M.F. de Groot [a], Krijn P. de Jong [a], Johannes H. Bitter [a,*]

[a] *Inorganic Chemistry and Catalysis, Department of Chemistry, Faculty of Sciences, Universiteit Utrecht, Sorbonnelaan 16, 3584 CA Utrecht, The Netherlands*

[b] *Shell Research and Technology Centre, Badhuisweg 3, 1031 CM, Amsterdam, The Netherlands*

Received 12 September 2006; received in revised form 28 November 2006; accepted 1 December 2006

Available online 29 December 2006

Abstract

The local structures of Ti doped $NaAlH_4$ were investigated with extended X-ray absorption fine structure (EXAFS) and X-ray absorption near edge structure (XANES) using $Ti(OBu)_4$ and $TiCl_3$ precursors. The local structures were linked to literature data on hydrogen desorption and absorption kinetics. In the $Ti(OBu)_4$ doped $NaAlH_4$, butoxide or decomposition products thereof (C, O atoms) was bonded to Ti after ball-milling, inhibiting the performance of the Ti catalyst. Upon heating, the C and O atoms were removed and Ti–Al species were formed. The thermodynamical most stable specie, $TiAl_3$, was not formed at $T < 300\,^{\circ}C$, contrarily to $TiCl_3$ doped $NaAlH_4$. Probably the initially present butoxide group gave rise to inhibition of its formation. Besides that, the butoxide or decompostion products thereof (C, O atoms) are also suspected to interfere with the hydrogen uptake of a desorbed $NaAlH_4$.

Keywords: Metal hydrides; EXAFS; XANES; Sodium alanate; Hydrogen storage

1. Introduction

Since the innovative work of Bogdanovic and Schwickardi from 1997 [1], hydrogen storage using Ti doped sodium alanate ($NaAlH_4$) has been subject of much research. This is mainly because sodium alanate displays suitable thermodynamic properties enabling reversible storage of hydrogen at low to medium temperatures suitable for mobile applications. The hydrogen is desorbed in two steps (Eqs. (1) and (2)) with respective equilibrium temperatures of 30 and 110 °C at 1 bar hydrogen pressure, and delivers a total of 5.6 wt% hydrogen storage capacity.

$$NaAlH_4 \leftrightarrow \tfrac{1}{3}Na_3AlH_6 + \tfrac{2}{3}Al + H_2 \quad (1)$$

$$Na_3AlH_6 \leftrightarrow \tfrac{1}{3}NaH + Al + \tfrac{1}{5}H_2 \quad (2)$$

The main difficulty to overcome for applying $NaAlH_4$ as a hydrogen storage material are the slow kinetics for hydrogen desorption and absorption. These unfavorable desorption and absorption rates can be improved by reducing the particle size of the $NaAlH_4$ to the nanometer range [2], or by adding a catalyst, for example $TiCl_3$ or Ti-butoxide, to the alanate [1,3,5]. Upon doping, the $TiCl_3$ precursor reacts to $NaAlH_4$ forming NaCl, Al, and a reduced Ti entity as shown in reaction (3) [5]. When $Ti(OBu)_4$ is used, the Ti is supposed to be reduced via reaction (4) [5].

$$TiCl_3 + 3NaAlH_4 \rightarrow \text{“Ti”} + 3Al + 3NaCl + 6H_2 \quad (3)$$

$$Ti(OBu)_4 + NaAlH_4 \rightarrow \text{“Ti”} + NaAl(OBu)_4 + 2H_2 \quad (4)$$

Several experimental studies reported that the Ti is finely dispersed, and is present as amorphous nano-particles in the $NaAlH_4$ or Al [6–9]. Therefore, characterization of the Ti on atomic scale is necessary, and suitable techniques are extended X-ray absorption fine structure (EXAFS) and X-ray absorption near edge structure (XANES).

It has been reported that the precursor has an influence on the initial hydrogen desorption and absorption properties, that is $TiCl_3$ doped $NaAlH_4$ display faster hydrogen desorption

* Corresponding author. Tel.: +31 302536778; fax: +31 302511027.
E-mail address: j.h.bitter@chem.uu.nl (J.H. Bitter).

0925-8388/$ – see front matter © 2006 Elsevier B.V. All rights reserved.
doi:10.1016/j.jallcom.2006.12.009

Table 1
Input parameters to create FEFF calculated Ti–Al, Ti–Ti, Ti–O and Ti–C references

	reference compound	S_0^2	σ^2 (10^3 Å^{-2})	V_r (eV)	V_i (eV)	Potential
Ti–Al	$TiAl_3$	0.72	1.50	11.3	1.0	Hedin-Lunqvist
Ti–Ti	*hcp* Ti foil	0.60	0.00	8.6	1.0	Hedin-Lunqvist
Ti–O	TiO_2 rutile	0.59	4.05	13.57	1.0	Hedin-Lunqvist
Ti–C	–	1.00	0.00	0	1.0	Hedin-Lunqvist

kinetics and also show enhanced hydrogen absorption rates compared to $Ti(OBu)_4$ doped $NaAlH_4$ [4,10,11]. Therefore, the proposed Ti entity after ball-milling $TiCl_3$ or $Ti(OBu)_4$ might not possess the same structure, and could be the origin of the difference in the initial kinetics. The atomic structure of Ti in $NaAlH_4$ has been investigated for $TiCl_3$ [6–9]. However the atomic structure has not been investigated for $Ti(OBu)_4$, and is presented here. The structures are investigated after ball-milling, in situ during hydrogen desorption of $NaAlH_4$, and will be compared to structural data obtained for $TiCl_3$ doped $NaAlH_4$.

2. Experimental

All sample preparations were performed under a nitrogen or argon atmosphere in a glovebox equipped with a circulation purifier. Commercially available $NaAlH_4$ (tech. 90% Sigma Aldrich) was purified and ball-milled with 10 mol% $TiCl_3$ and 12 mol% $Ti(OBu)_4$ as described before [4]. These samples are referred to as $TiCl_3/NaAlH_4$ and $Ti(OBu)_4/NaAlH_4$. One part of the $TiCl_3/NaAlH_4$ was heated in Ar to 225 °C with a ramp of 5 °C/min until no detectable hydrogen desorption was recorded by volumetric analysis ($TiCl_3/NaAlH_4$-225). The $Ti(OBu)_4/NaAlH_4$ was desorbed in situ to 90 °C, kept isothermal for 30 min, and cooled down ($Ti(OBu)_4/NaAlH_4$-90). Next, the sample was desorbed at 150 °C isothermal for 12 h ($Ti(OBu)_4/NaAlH_4$-150). After that, the temperature was increased to 300 °C and kept isothermal for 30 min ($Ti(OBu)_4/NaAlH_4$-300).

X-ray absorption spectroscopy was performed on the Ti K-edge at station E4 of the DESY synchrotron (Hamburg, Germany), using a Si (1 1 1) double crystal monochromator that was detuned to 80% to suppress higher harmonics. All measurements were performed at 77 K in flowing He to exclude thermal decomposition of the sample. The samples (11 mg of Ti-doped $NaAlH_4$) were homogeneously diluted with 50 mg BN, pressed in a pellet, mounted to the cell and transferred to the beam-line in a closed cell under inert atmosphere.

Extraction of the EXAFS data was performed as described elsewhere [12]. The Ti–Al backscattering amplitude and phase shift were calculated using the FEFF 8.2 code [13] and calibrated using an experimental measured spectrum at 77 K so that E_0 and σ^2 of the references were zero. The FEFF input parameters, and used references are listed in Table 1. Experimental data were fitted in k^2 using the difference file technique in R-space from $3 < k < 10$ or $3 < k < 12$ (Å^{-1}) depending on the quality of the data. The quality of the fit was checked by applying k^1, k^2 and k^3 weightings.

XANES was recorded from 4950 to 5050 eV with a stepsize of 0.3 eV. The position of the edge was set at the maximum of the first derivative (inflection point) of the absorption edge. Spectra were normalized to 5020 eV.

3. Results

The magnitude of the uncorrected Fourier Transform (FT) of $Ti(OBu)_4/NaAlH_4$ and $TiCl_3/NaAlH_4$ treated at various temperatures are shown in Fig. 1. It is observed that the FT changed significantly upon changing temperature and/or precursor. The changes were quantified in the fits of the different samples. The k^2 variances of the fits (Table 2) are low, indicating that the fits were of a comparable good quality. The fit parameters of $Ti(OBu)_4/NaAlH_4$ are listed in Table 2. It was observed that 4.5 oxygen atoms surrounded Ti in its closest shell at 1.99 Å, which is a typical distance for Ti-oxides [14]. The next shell contained 3.4 Ti–C bonds at 2.49 Å. This distance is relatively long for a Ti–C distance, which is typically at 2.1–2.2 Å [15]. However, Ti–C distances of ~2.4 Å have been reported before [15]. No atoms were observed in higher shells.

After heating $Ti(OBu)_4/NaAlH_4$ to 90 °C, the distances of the first two shells altered only slightly. In contrast, the coordination number decreased in both samples from 4.5 to 1.9 (Ti–O), and from 3.4 to 1.9 (Ti–C). Besides that, the third shell displayed an Al atom at 2.82 Å, which was at a typical distance for Ti–Al bonds in Ti doped $NaAlH_4$ systems [6–9]. After heating the sample to 150 °C, the nearest shells did not contain O or C atoms (Table 2 $Ti(OBu)_4/NaAlH_4$-150). The fit parameters show that two Al atoms surrounded the Ti at 2.76, 2.92 Å,

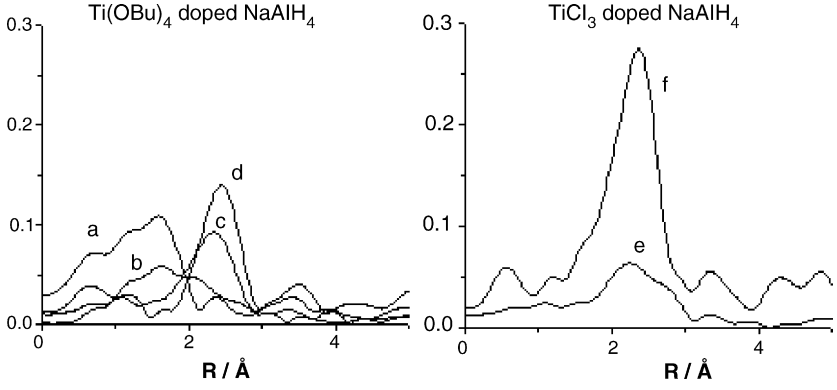

Fig. 1. Magnitude of Fourier transformed $\chi(k)$: (a) $Ti(OBu)_4/NaAlH_4$, (b) $Ti(OBu)_4/NaAlH_4$-90, (c) $Ti(OBu)_4/NaAlH_4$-150, (d) $Ti(OBu)_4/NaAlH_4$-300, (e) $TiCl_3/NaAlH_4$, (f) $TiCl_3/NaAlH_4$-225. (k^1; Δk; 3–12 Å^{-1}).

Table 2
EXAFS fits of $Ti(OBu)_4$ doped $NaAlH_4$ after ball-milling, and after desorption at 90 °C, 150 °C

Name	Fit range (Å)	Shell	Atom	N	$\Delta\sigma^2$ (10^3 Å^{-2})	R (Å)	E_0 (eV)	k^2-variance	
								Im.	Abs.
$Ti(OBu)_4/NaAlH_4$	1.1–2.1	1	Ti–O	4.5	8.60	1.99	3.09	0.24	0.17
		2	Ti–C	3.4	0.88	2.48	−0.60		
$Ti(OBu)_4/NaAlH_4$-90	1.0–2.8	1	Ti–O	1.9	1.78	1.91	2.40	0.40	1.02
		2	Ti–C	1.9	0.57	2.52	−7.00		
		3	Ti–Al	1.5	3.22	2.83	−1.05		
$Ti(OBu)_4/NaAlH_4$-150	1.8–3.6	1	Ti–Al	3.3	0.51	2.76	−1.32	0.07	0.10
		2	Ti–Al	2.0	0.50	2.92	0.57		
		3	Ti–Ti	1.3	0.83	3.39	4.06		
$Ti(OBu)_4/NaAlH_4$-300	1.9–3.3	1	Ti–Al	6.7	0.60	2.82	−1.65	0.46	0.25
		2	Ti–Al	3.0	0.50	3.00	4.91		
		3	Ti–Ti	2.0	3.60	3.39	8.83		
$TiCl_3/NaAlH_4$	1.2–3.5	1	Ti–Al	2.3	0.04	2.71	−0.96	0.63	0.40
		2	Ti–Al	2.5	0.18	2.89	0.96		
		3	Ti–Ti	1.9	0.81	3.52	1.93		
$TiCl_3/NaAlH_4$-225	1.2–3.5	1	Ti–Al	4.6	0.10	2.73	1.53	0.36	0.23
		2	Ti–Al	7.8	0.82	2.84	4.97		
		3	Ti–Ti	3.8	6.36	3.90	4.31		

which are at typical distances for $TiAl_x$ alloys [6–9,16]. Further heating increased the Ti–Al bond distances slightly, however the coordination number of Ti–Al increased significantly from 3.3 to 6.7, and 2.0 to 3.0 Al atoms in the nearest shells.

The local structure for $TiCl_3/NaAlH_4$ is listed in Table 2, and it is observed that Al surrounded the Ti. A detailed description of this structure can be found in an upcoming article [9]. After heating to 225 °C ($TiCl_3/NaAlH_4$-225), the local structure was similar to the local structure of $TiAl_3$, that is 4 Al atoms at 2.73 Å, 8 Al atoms at 2.84 Å, and 4 Ti atoms at 3.90 Å.

The XANES of several samples are shown in Fig. 2. The edge positions of all measured samples are listed in Table 3. The first feature in the Ti edge for Ti-oxides, is a pre-edge feature [17] and the edge position was determined at the inflection point of the second rising edge for the samples that contained oxygen, that is $Ti(OBu)_4/NaAlH_4$ and TiO_2. For the samples

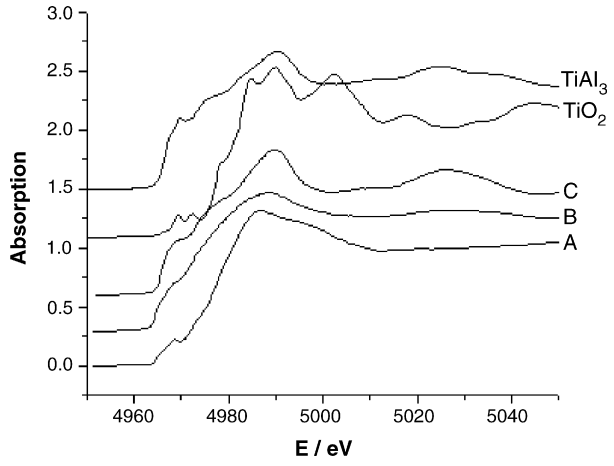

Fig. 2. XANES of (A) $Ti(OBu)_4/NaAlH_4$, (B) $Ti(OBu)_4/NaAlH_4$-150, (C) $TiCl_3/NaAlH_4$-225, and references TiO_2 and $TiAl_3$.

Table 3
Positions of Ti-edges in SAH-start, SAH-125, SAH-225, SAH-475 and $TiAl_3$

	Edge position (eV)
$TiCl_3/NaAlH_4$	4965.7
$TiCl_3/NaAlH_4$-225	4966.1
$Ti(OBu)_4/NaAlH_4$	4972.3
$Ti(OBu)_4/NaAlH_4$-90	–
$Ti(OBu)_4/NaAlH_4$-150	4967.0
$Ti(OBu)_4/NaAlH_4$-300	4967.0
TiO_2	4976.5
$TiAl_3$	4966.7
Ti foil	4965.5

that did not contain oxygen, the first rising edge was taken as the absorption edge. No edge energy has been determined for $Ti(OBu)_4/NaAlH_4$-90, as EXAFS fit indicated that local structure involved both oxygen and aluminum atoms, and the absorption edge consists probably of a combination of two oxidation states. It was also observed that the resonances of $Ti(OBu)_4/NaAlH_4$ and $Ti(OBu)_4/NaAlH_4$-150 were less pronounced than the resonances of crystalline references $TiAl_3$ and TiO_2 (Fig. 2).

4. Discussion

The position of the Ti absorption edge energy represents the oxidation state of Ti in Ti-butoxide doped $NaAlH_4$. Table 3 shows that the position of the edge energy was significantly higher for $Ti(OBu)_4/NaAlH_4$ than the position of the edge in Ti-metal. The shift in edge energy is linearly dependant of the oxidation state of Ti (◯ symbols in Fig. 3) [6]. Note that the edge shift of TiO_2 differs 3 eV with TiO_2 obtained from literature, probably due to differences in determining the edge energy. Assuming a linear relationship between oxidation state and edge

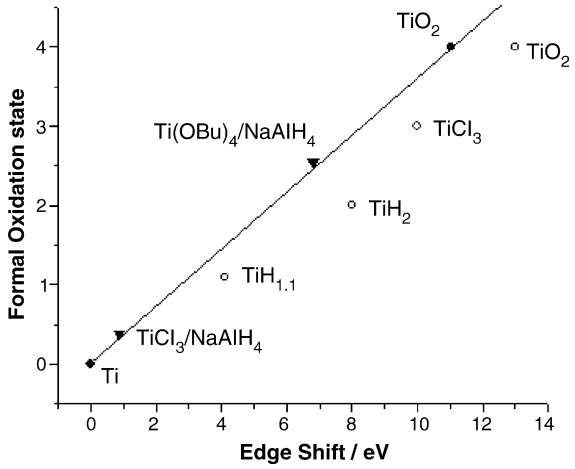

Fig. 3. Shift in Ti K-edge, ● measured references, used to calibrate samples with unknown valency (▼), ◯ Ti standards taken from [6].

shift of our recorded Ti-metal and TiO_2 (Fig. 3), it is calculated that the formal valency of Ti was +2.5 in $Ti(OBu)_4/NaAlH_4$ after ball-milling. These findings are in contradiction with the doping reaction between $Ti(OBu)_4$ and $NaAlH_4$ reaction (4), in which the Ti is claimed to be reduced to Ti^0. Contrarily, when doping with $TiCl_3$ the oxidation state was +0.3 ($TiCl_3/NaAlH_4$), and indicated that the Ti was reduced to a low oxidation state in the doping process (Fig. 3). It was also observed that the XANES resonances of $Ti(OBu)_4$ doped $NaAlH_4$ were damped compared to crystalline materials such as $TiAl_3$ and TiO_2 (Fig. 2). Similar damped resonances were reported and explained by Graetz et al. by presence of surface nano-entities [6]. Probably, in the case of $Ti(OBu)_4/NaAlH_4$ the Ti is highly dispersed on the $NaAlH_4$.

To further investigate the structures of these highly dispersed Ti-particles, the local structures were determined with EXAFS. The EXAFS fit parameters in Table 2 revealed that Ti was surrounded by oxygen and carbon atoms after ball-milling $Ti(OBu)_4$ with $NaAlH_4$. The carbon and oxygen atoms originated from the decomposition of the butoxide group of the Ti-precursor, thus most probably the Ti was not in the close vicinity of the $NaAlH_4$ in this stage of the experiment. Upon heating to 90 °C, the coordination number of the Ti–O and Ti–C shells decreased from 4.5 to 1.9 (Ti–O), and 3.4 to 1.9 (Ti–C). This indicates that the C and O atoms of the Ti were removed for approximately 50% during this temperature treatment. At the same time Ti–Al scattering at 2.82 Å appeared from the fit (Table 2). This indicates that the heat treatment partly broke the oxygen and carbon bonds, and Ti reacted with the formed Al metal (as $NaAlH_4$ decomposed to NaH and Al metal). This process prolonged when the sample was heated to 150 °C. Namely, in $Ti(OBu)_4/NaAlH_4$-150, no Ti–O or Ti–C bonds were detected in the closest coordination spheres (Table 2), and the Ti was surrounded by Al at 2.76 and 2.92 Å. The coordination number of Al was low (3.3 + 2.0 = 5.3), since a crystalline $TiAl_3$ alloy has 4 + 8 = 12 Al neighbors. Presumably, the Ti is present as Ti–Al nano entities as was also inferred from XANES. As a result, the Ti–O–C that was present in the pristine sample was probably converted to an Na–Al–O–C–H phase. The coordination number of Al increased further when the sample was heated to 300 °C ($Ti(OBu)_4/NaAlH_4$-300), but the local structure was dissimilar to $TiAl_3$.

In the EXAFS fits of $TiCl_3$ milled $NaAlH_4$, the chloride precursor ion did not appear in the fits (Table 2), and only Ti–Al distances were observed in the first two shells. This illustrates that Ti in $TiCl_3$ was more easily reduced than Ti in $Ti(OBu)_4$. When $TiCl_3/NaAlH_4$ was heated to 225 °C ($TiCl_3/NaAlH_4$-225) the local structure was identical to the local structure of $TiAl_3$, and contained 4 + 8 = 12 Al atoms. This indicates that thermodynamical lowest state ($TiAl_3$) had been reached. After heating the Ti in $Ti(OBu)_4$ doped $NaAlH_4$, the Ti enriched with Al atoms. However, its first coordination sphere contained 3 + 6.7 = 9.7 Al atoms after the final temperature treatment to 300 °C ($Ti(OBu)_4/NaAlH_4$-300). Thus, the Ti was not fully surrounded by Al atoms in this sample, and did not reach the thermodynamical lowest state ($TiAl_3$ alloy). Apparently, the thermodynamical lowest state was reached slower with $Ti(OBu)_4$ precursor than using $TiCl_3$.

Several reports indicate that the hydrogen desorption rates are faster for the $TiCl_3$ dopant than for $Ti(OBu)_4$, and this has also been confirmed for our investigated samples (not shown) [4,10,11]. It was observed that the oxidation state of the Ti was +2.5 in $Ti(OBu)_4/NaAlH_4$ and +0.3 in $TiCl_3/NaAlH_4$ (Fig. 3). It might be that the oxidation state of Ti is of crucial importance for its catalytic performance. Another, related, explanation is that the butoxide group occupies space around Ti, and shields the Ti from $NaAlH_4$ leading to a lesser active Ti-catalyst.

Besides improved desorption rates, hydrogen absorption rates and capacities are also better using $TiCl_3$ than Ti-butoxide [4]. The coordination number of Al around Ti is low in $Ti(OBu)_4/NaAlH_4$-150, which is a sign that Ti particles were small and/or at the surface. In contrast, the coordination number for $TiCl_3$ doped $NaAlH_4$ is higher, but still displays better absorption rates and capacities [4,9]. As Ti–Al surface or nano entities are considered as the active species [6–9], this kinetic difference cannot be explained on basis of EXAFS/XANES results. As concluded before, the butoxide groups were removed from the Ti, but an in situ gas phase IR experiment did not indicate presence of hydrocarbons upon heating $Ti(OBu)_4/NaAlH_4$ to 450 °C. Thus, the butoxide must have reacted with $NaAlH_4$, NaH or Al. The ratio of carbon to aluminum is high (C/Al ratio = 1.9), and interferes most likely with H_2 absorption process, that is Ti-catalyst is blocked by remaining C and O atoms.

5. Conclusions

Doping $Ti(OBu)_4$ and $TiCl_3$ under identical conditions yields different Ti species. For $TiCl_3$, Ti was reduced to $Ti^{0.3}$, whereas for $Ti(OBu)_4$ the Ti oxidation state was +2.5, and the butoxide groups and/or C and O atoms were detected around Ti. The presence of carbon and oxygen inhibited the Ti catalyst for hydrogen desorption. The butoxide groups were removed in between 90 and 150 °C, and delayed the formation of the thermodynamical most stable state ($TiAl_3$ alloy) compared to when a more easily reducible Ti-agent, $TiCl_3$, was used. The presence of carbon and oxygen atoms in the bulk interferes possibly with hydrogen uptake and the activity of the Ti-catalyst.

Acknowledgements

This work was financially supported by ACTS, project number 053.61.02, and HASYLAB project number I-05-062 EC. We thank Dr. Konstantin Klementiev from HASYLAB for providing $TiAl_3$. We also thank F. Soulimani from Utrecht University for assistance during the IR-experiment.

References

[1] B. Bogdanovic, M. Schwickardi, J. Alloys Compd. 253–254 (1997) 1–9.
[2] C.P. Baldé, B.P.C. Hereijgers, J.H. Bitter, K.P. de Jong, Angew. Chem. Int. Ed. 45 (2006) 3501–3503.
[3] C.M. Jensen, R.A. Zidan, N. Mariels, A.G. Hee, C. Hagen, Int. J. Hydrogen Energy 24 (1999) 461.
[4] A.G. Haiduc, H.A. Stil, M.A. Schwarz, P. Paulus, J.J.C. Geerlings, J. Alloys Compd. 393 (2005) 252–263.
[5] J.M. Bellosta von Colbe, B. Bogdanovic, M. Felderhof, A. Pommerin, F. Schüth, J. Alloys Compd. 370 (2004) 104–109.
[6] J. Graetz, J.J. Reilly, J. Johnson, A.Y. Ignatov, T.A. Tyson, Appl. Phys. Lett. 85 (2004) 500–502.
[7] M. Felderhoff, K. Klementiev, W. Grunert, B. Spliethoff, B. Tesche, J.M. Bellosta Von Colbe, B. Bogdanovic, M. Hartel, A. Pommerin, F. Schüth, C. Weidenthaler, Phys. Chem. Chem. Phys. 6 (2004) 4369–4374.
[8] A. Léon, O. Kircher, J. Rothe, M. Fichtner, J. Phys. Chem. B 108 (2004) 16372–16376.
[9] C.P. Baldé, H.A. Stil, A. M.J. van der Eerden, K.P. de Jong, J.H. Bitter, J. Phys. Chem. C, in press.
[10] B. Bogdanovic, R.A. Brand, A. Marjanovic, M. Schwickardi, J. Tölle, J. Alloys Compd. 302 (2000) 36–58.
[11] F. Schüth, B. Bogdanovic, M. Felderhof, Chem. Commun. 37 (2004) 2249–2258.
[12] D.C. Koningsberger, B.L. Mojet, G.E. Van Dorssen, D.E. Ramaker, Top. Catal. 10 (2000) 143–155.
[13] S.I. Zabinsky, J.J. Rehr, A.L. Ankudinov, R.C. Albers, H.J. Eller, Phys. Rev. B: Condens. Matter 52 (1995) 2995.
[14] L. Vegard, Philos. Mag. 32 (1916) 505–518.
[15] E.P. Wasserman, A.D. Westwood, Z. Yu, J.H. Oskam, S.L. Duenas, J. Mol. Catal. A: Chem. 172 (2001) 67–80.
[16] P. Norby, A.N. Christensen, Acta Chem. Scand., Series A 40 (1986) 157–159.
[17] F. Farges, G.E. Brown Jr., J.J. Rehr, Phys. Rev. B: Condens. Matter 56 (1997) 1809–1819.